BIOCHEMISTRY
including biophysical chemistry & molecular biology

Article

pubs.acs.org/biochemistry

Domain Swapping of the Heme and N-Terminal α-Helix in *Hydrogenobacter thermophilus* Cytochrome c_{552} Dimer

Yugo Hayashi,[†] Satoshi Nagao,[†] Hisao Osuka,[‡] Hirofumi Komori,[‡,§] Yoshiki Higuchi,[‡,§] and Shun Hirota*[,†]

[†]Graduate School of Materials Science, Nara Institute of Science and Technology, 8916-5 Takayama, Ikoma, Nara 630-0192, Japan

[‡]Department of Life Science, Graduate School of Life Science, University of Hyogo, 3-2-1 Koto, Kamigori-cho, Ako-gun, Hyogo 678-1297, Japan

[§]RIKEN SPring-8 Center, 1-1-1 Koto, Sayo-cho, Sayo-gun, Hyogo 679-5148, Japan

Supporting Information

ABSTRACT: Oxidized horse cytochrome *c* (cyt *c*) has been shown to oligomerize by domain swapping its C-terminal helix successively. We show that the structural and thermodynamic properties of dimeric *Hydrogenobacter thermophilus* (HT) cytochrome c_{552} (cyt c_{552}) and dimeric horse cyt *c* are different, although both proteins belong to the cyt *c* superfamily. Optical absorption and circular dichroism spectra of oxidized dimeric HT cyt c_{552} were identical to the corresponding spectra of its monomer. Dimeric HT cyt c_{552} exhibited a domain-swapped structure, where the N-terminal α-helix together with the heme was exchanged between protomers. Since a relatively strong H-bond network was formed at the loop around the heme-coordinating Met, the C-terminal α-helix did not dissociate from the rest of the protein in dimeric HT cyt c_{552}. The packing of the amino acid residues important for thermostability in monomeric HT cyt c_{552} were maintained in its dimer, and thus, dimeric HT cyt c_{552} exhibited high thermostability. Although the midpoint redox potential shifted from 240 ± 2 to 213 ± 2 mV by dimerization, it was maintained relatively high. Ethanol has been shown to decrease both the activation enthalpy and activation entropy for the dissociation of the dimer to monomers from 140 ± 9 to 110 ± 5 kcal/mol and 310 ± 30 to 270 ± 20 cal/(mol·K), respectively. Enthalpy change for the dissociation of the dimer to monomers was positive (14 ± 2 kcal/mol per protomer unit). These results give new insights into factors governing the swapping region and thermodynamic properties of domain swapping.

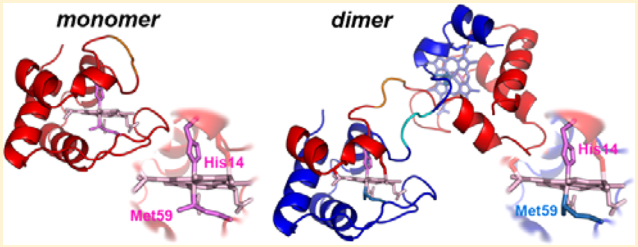

Protein forms a native structure according to its amino acid sequence.[1] However, under specific conditions, proteins may suffer structural changes, which may cause protein misfolding diseases.[2−4] Oligomerization of proteins has gained interest as initial intermediates of amyloid fibril formation,[4−6] and domain swapping has been detected in oligomerization of several amyloidogenic proteins.[7−10] Domain swapping is a phenomenon where one molecule exchanges its domain or secondary structural element with another molecule. The number of proteins identified with domain-swapped structures has been increasing,[5,11−13] and domain-swapped structures have also been reported for several heme proteins.[14−17] Runaway (successive) domain swapping has been suggested as a mechanism for polymerization of serpin,[18,19] as well as for formation of RNase A fibrils (3D domain-swapped zipper-spine model).[5,20] Successive domain swapping has also been suggested for human γD-crystallin by molecular dynamics simulation.[21] We have recently shown that horse cyt *c* also forms polymers by successive domain swapping the C-terminal α-helix, where this α-helix was displaced from its original position in the monomer.[22] In dimeric horse cyt *c*, Met80 was dissociated from the heme iron, and a higher peroxidase activity was observed in the dimer compared to its monomer.[22,23]

Cytochrome c_{552} (cyt c_{552}) belongs to the cyt *c* superfamily. *Pseudomonas nautica* cyt c_{552} has been proposed to be an electron donor for cytochrome cd_1,[24] although the function of thermophilic *Hydrogenobacter thermophilus* (HT) cyt c_{552} is not known. HT cyt c_{552} is smaller than mammalian cyt *c* and consists of 80 amino acids (9.2 kDa).[25] HT cyt c_{552} contains three long α-helices similar to other proteins in the cyt *c* superfamily, and His14 and Met59 are coordinated to its heme iron.[25,26] The denaturation temperature (T_d) of oxidized HT cyt c_{552} is higher than 100 °C.[27] The high thermostability of HT cyt c_{552} has been attributed to the packing of the hydrophobic residues responsible for the increased hydrophobic interaction by comparison with the structure of mesophilic *Pseudomonas aeruginosa* (PA) cyt c_{551}, whose amino acid sequence matches 56% of that of HT cyt c_{552}.[28−33] The T_d of the oxidized and reduced forms of HT cyt c_{552} are higher by about 27 and 20 °C, respectively, than those of the corresponding forms of PA cyt c_{551}, and the midpoint redox potential (E_m) of HT cyt c_{552} is

Received: August 21, 2012
Revised: October 2, 2012
Published: October 4, 2012

dx.doi.org/10.1021/bi3011303 | *Biochemistry* 2012, 51, 8608−8616

lower by about 60 mV than that of PA cyt c_{551}.[32,34] It has been suggested from these results that the redox function of HT cyt c_{552} is enthalpically regulated through the stability of the oxidized form. However, heme-depleted HT cyt c_{552} has been shown to form amyloid fibrils,[35] as well as cyt *c*.[36]

It has been assumed that because the monomer and domain-swapped dimer share the same structures except the hinge loop, the free energy difference between closed and open monomers for domain swapping is small with a high energy barrier in between.[37,38] This energy barrier can be reduced by a change in pH,[37] mutation in the protein,[39−42] and treatment with denaturants.[22,38,41,43] It has been proposed that RNase A forms domain-swapped dimers and trimers by opening the N- or C-terminal segments under certain conditions.[38,43−45] Recently, it has been shown with NMR spectroscopy that RNase A oligomers are formed by refolding from a chiefly denatured state.[46] However, information on the factors governing the swapping region and the thermodyanamic properties of domain swapping are limited. We show that dimeric HT cyt c_{552} is formed by domain swapping the N-terminal α-helical region containing the heme. In contrast to horse cyt *c*, the C-terminal α-helix did not dissociate from the rest of the protomer in dimeric HT cyt c_{552}, presumably because of the stiffness of the Gly49−Thr65 loop containing the heme-coordinating Met59. We also found that dimeric HT cyt c_{552} is enthalpically favored compared to its monomer.

MATERIALS AND METHODS

Protein Purification and Oligomerization. HT cyt c_{552} was expressed in *Escherichia coli* and purified as reported previously.[28,29] The oxidized form of the protein was prepared by an addition of potassium ferricyanide.

Oxidized dimeric HT cyt c_{552} was prepared by dissolving oxidized HT cyt c_{552} (200 μM) in 50 mM sodium phosphate buffer, pH 7.0, followed by addition of ethanol (final concentration, 80% (v/v)) at 0−50 °C. After centrifugation of the HT cyt c_{552} solution, the precipitate was lyophilized to remove residual ethanol. The lyophilized precipitate was dissolved in 50 mM sodium phosphate buffer, pH 7.0, at 4 °C. The solution containing oxidized dimeric HT cyt c_{552} was incubated at 80 °C for 1 h. After the incubation, dimeric HT cyt c_{552} was purified by gel chromatography (HiLoad 26/60 Superdex75, GE healthcare, Buckinghamshire) using a fast protein liquid chromatography (FPLC) system (BioLogic DuoFlow 10, Bio-Rad, CA) several times with the same buffer at 4 °C. The absorption coefficients of the oxidized monomer and dimer were obtained with the pyridine hemochrome method.[47] The concentrations of the proteins were calculated from the absorbance at 410 nm with these absorption coefficients, and adjusted to desired concentrations.

To investigate formation of oxidized monomeric HT cyt c_{552} from its dimer by treatment with ethanol, a 500 μL solution of dimeric HT cyt c_{552} (heme, 10 μM) in 50 mM sodium phosphate buffer, pH 7.0, was mixed with 2 mL of ethanol (final concentration, 80% (v/v)) at 50 °C, where precipitates were obtained. After lyophilization of the produced precipitates, the precipitates were dissolved in 500 μL of 50 mM sodium phosphate buffer, pH 7.0, at 4 °C. The stability of oxidized dimeric HT cyt c_{552} was investigated by incubation of the purified dimer (heme, 10 μM) in 50 mM sodium phosphate buffer, pH 7.0, containing 100 μM ferricyanide in the presence and absence of 60% (v/v) ethanol at 36−43 °C and 82.5−92 °C, respectively.

Formation of dimeric HT cyt c_{552} in the presence of ethanol was investigated by addition of ethanol (final concentration, 60% (v/v)) to oxidized monomeric HT cyt c_{552} (40 μM) in 10 mM sodium phosphate buffer, pH 7.0, at 20 and 50 °C, and subsequent incubation for 1 min at the same temperature. After the incubation, the protein solution (500 μL) was mixed with 50 mM sodium phosphate buffer (3 mL), pH 7.0, at 4 °C. The mixed solution was concentrated and analyzed by gel chromatography.

Size Exclusion Chromatographic Analysis. The oligomeric HT cyt c_{552} solutions were analyzed by gel chromatography (column: Superdex 75 30/100 GL, GE healthcare) using the FPLC system (BioLogic DuoFlow 10, Bio-Rad) with 50 mM sodium phosphate buffer, pH 7.0, at 4 °C. The peak areas in the elution curves of gel chromatography were obtained by least-squares fitting the peaks with Gaussian curves using the Igor Pro 6.0 software package (WaveMetrics, Portland).

Optical Absorption and Circular Dichroism Measurements. Optical absorption spectra were measured with a UV-2450 spectrophotometer (Shimadzu, Japan) using a 1-cm-path-length quartz cell at 20 °C. Circular dichroism (CD) spectra were measured with a J-725 CD spectropolarimeter (Jasco, Japan) using a 0.1-cm-path-length quartz cell at room temperature.

X-ray Crystallographic Analysis. Crystallization was carried out at room temperature using the sitting drop vapor diffusion method with crystal plates (CrystalClear D Strips, Douglas Instruments, Hampton Research, CA). Oxidized dimeric HT cyt c_{552} was dissolved in 100 mM HEPES buffer, pH 7.0, at a protein concentration of 18.4 mg/mL. Droplets prepared by mixing 1 μL of the protein solution with 1 μL reservoir solution were equilibrated. The best reservoir solution was found to be 100 mM HEPES buffer, 800 mM ammonium sulfate, and 45% (v/v) 2-methyl-2,4-pentanediol, pH 7.0.

The diffraction data were collected at the BL38B1 beamline at SPring-8, Japan. The crystal was mounted on a cryo-loop and flash-frozen at 100 K in a nitrogen cryo system, Quantum315 (ADSC). The crystal to detector distance was 200 mm, and the wavelength was 1.0 Å. The oscillation angle was 1°, and exposure time was 7 s per frame. The total number of frames was 180. The diffraction data were processed using the program, HKL2000.[48]

The preliminary structure was obtained by a molecular replacement method (MOLREP) using the atomic coordinates of the structure of monomeric HT cyt c_{552} (PDB code: 1YNR) as a starting model. The structure refinement was performed using the program, REFMAC. The molecular model was manually corrected, and water molecules were picked up in the electron density map using the program, COOT. The data collection and refinement statistics are summarized in Table S1, Supporting Information.

Electrochemistry. Cyclic voltammetry responses were obtained with an ALS-612DN electrochemical analyzer (BAS Inc., Tokyo, Japan). An Au electrode was used as a working electrode. A Pt wire and Ag/AgCl (3 M NaCl) were used as counter and reference electrodes, respectively. The potentials were referred to the normal hydrogen electrode (NHE). Modification of the Au electrode surface was performed by the following procedure. The Au electrode was polished with 0.05 μm alumina water slurry, rinsed with purified water to remove residual organic compounds from the electrode surface, and cleaned by electrochemical oxidation/reduction treatment.[49] The Au electrode was dipped in purified water containing 1

dx.doi.org/10.1021/bi3011303 | *Biochemistry* 2012, 51, 8608−8616

mM 4-mercaptopyridine (Wako, Osaka, Japan) for 30 s, and subsequently rinsed with purified water. Cyclic voltammograms of monomeric and dimeric HT cyt c_{552} (heme, 200 μM) were recorded in 50 mM sodium phosphate buffer, pH 7.0. All measurements were performed with a scan rate of 50 mV/s at room temperature, after degassing with a vacuum line and flowing Ar gas for at least 5 min to remove oxygen from the solution.

Differential Scanning Calorimetric Measurements. Differential scanning calorimetry (DSC) thermograms of monomeric and dimeric HT cyt c_{552} (heme, 100 μM) were measured using VP-DSC (MicroCal, GE Healthcare) at a scan rate of 1 °C/min with 50 mM sodium phosphate buffer, pH 7.0.

RESULTS

Formation of Oligomeric HT Cyt c_{552}. Oxidized HT cyt c_{552} in 10 mM sodium phosphate buffer, pH 7.0, precipitated with addition of ethanol (final concentration, 80% (v/v)) at all temperatures investigated (0–50 °C). After the precipitate was lyophilized to remove residual ethanol, it was dissolved in 50 mM sodium phosphate buffer, pH 7.0. Monomeric HT cyt c_{552} was observed at about 14 mL in the elution curves of size exclusion chromatography of the ethanol-treated HT cyt c_{552} solutions when we used a Superdex 75 10/300 GL column (Figure S1, Supporting Information). Only a small amount of dimeric HT cyt c_{552} was detected after treatment in 80% (v/v) ethanol at 20 °C. By the same treatment at 35 °C, peaks corresponding to dimeric and trimeric HT cyt c_{552} were detected at about 12.5 and 11.6 mL, respectively, in addition to the monomer peak (Figure S1, Supporting Information). The relative intensities of the oligomer peaks in the elution curves of size exclusion chromatography increased as the temperature during addition of ethanol to the precipitates was increased from 0 to 50 °C (Figure S1, Supporting Information).

Precipitates were also obtained when oxidized dimeric HT cyt c_{552} was treated with 50 mM sodium phosphate buffer, pH 7.0, containing 80% (v/v) ethanol at 50 °C. These precipitates contained monomers, indicating that dimers dissociate to monomers by addition of ethanol (Figure S2, curve d, Supporting Information). The precipitates also contained trimers and tetramers. The intensity of the dimer peak decreased more than 70% by addition of 80% (v/v) ethanol at 50 °C. These results indicate that ethanol may induce structural changes in dimeric HT cyt c_{552}, and the conversion between the monomer and dimer is reversible in the presence of ethanol. Reversibility of oligomerization has also been observed in horse cyt c in the presence of ethanol.[22]

Structure of Dimeric HT Cyt c_{552}. The structural properties of dimeric HT cyt c_{552} were investigated to reveal the structural basis of dimerization. The maximum wavelength of the Soret band of oxidized dimeric HT cyt c_{552} was detected at 410 nm (Figure 1A), which was similar to that of the oxidized monomer.[50] The absorption coefficient of the dimer Soret band at 410 nm was obtained as 113000 ± 3000 M^{-1} cm^{-1} (heme unit) with the pyridine hemochrome method.[47] This value was similar to that obtained for the monomer, 109000 ± 2000 $M^{-1}cm^{-1}$, which was close to the reported value (105000 M^{-1} cm^{-1} at 409.5 nm).[51] It has been reported that the 690-nm absorption band of oxidized HT cyt c_{552} is related to the coordination of Met59 to the heme iron.[52] The intensity of the 690-nm band of the dimer was also similar to that of the monomer (Figure 1A), indicating that Met59 is

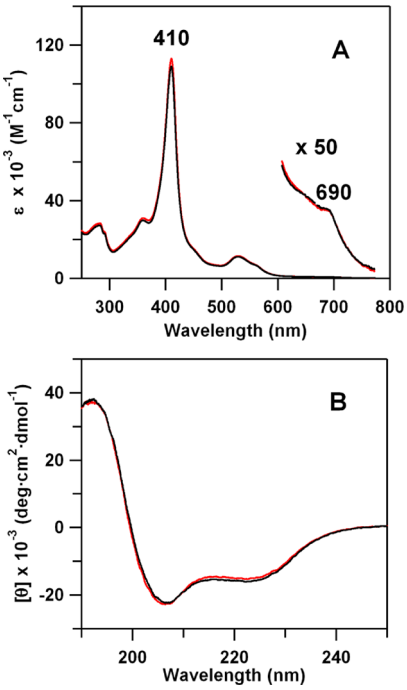

Figure 1. Optical absorption and CD spectra of oxidized monomeric and dimeric HT cyt c_{552}. (A) Spectra of oxidized monomeric (black) and dimeric (red) HT cyt c_{552}. The spectra near the 690-nm band are expanded 50 times. (B) CD spectra of oxidized monomeric (black) and dimeric (red) HT cyt c_{552}. The concentration of the protein was calculated from the intensity of its Soret band. Measurement conditions: Sample concentration (heme): (A) 16–17 μM, (B) 9 μM; solvent: 50 mM sodium phosphate buffer; pH: 7.0; temperature: (A) 20 °C, (B) room temperature.

coordinated to the heme iron in the dimer. In the CD spectrum of oxidized dimeric HT cyt c_{552}, negative peaks were observed at 208 and 222 nm, whose intensities were similar to those of the monomer (Figure 1B). These similarities in the spectroscopic properties between monomeric and dimeric HT cyt c_{552} indicate that the active site and secondary structures of the monomer and dimer are similar.

To elucidate the detailed structure of dimeric HT cyt c_{552}, we solved the X-ray crystal structure of dimeric HT cyt c_{552} (PDB ID: 3VYM). The structure of dimeric HT cyt c_{552} at 2.0 Å resolution exhibited a domain-swapped structure, where the positions of Ala18, Lys19, and Lys20 in the dimer were relocated from those in the monomer (Figure 2). The N-terminal α-helix from Asn1 to Lys17 together with the heme was exchanged with the corresponding region of another molecule (Figure 2). It is noteworthy that the swapped region in dimeric HT cyt c_{552} was different from that in dimeric horse cyt c.[22]

Met59 coordinated to the heme in dimeric HT cyt c_{552}, but the Met originated from the other protomer to which the heme belonged (Figure 3). Between the monomer and dimer, a change in the orientation of the terminal CH_3 group of the Met side chain was observed (Figure 3). The Fe–His14 and Fe–Met59 distances of dimeric HT cyt c_{552} were 1.89 and 2.28 Å, which were shorter than the corresponding distances in the monomer (Fe–His14, 2.05–2.09 Å; Fe–Met59, 2.33–2.40 Å) (Table 1).

There is one HT cyt c_{552} protomer in the asymmetric unit of the crystal of the dimer. The overall protein structure corresponds very well between the monomer and dimer

dx.doi.org/10.1021/bi3011303 | Biochemistry 2012, 51, 8608–8616

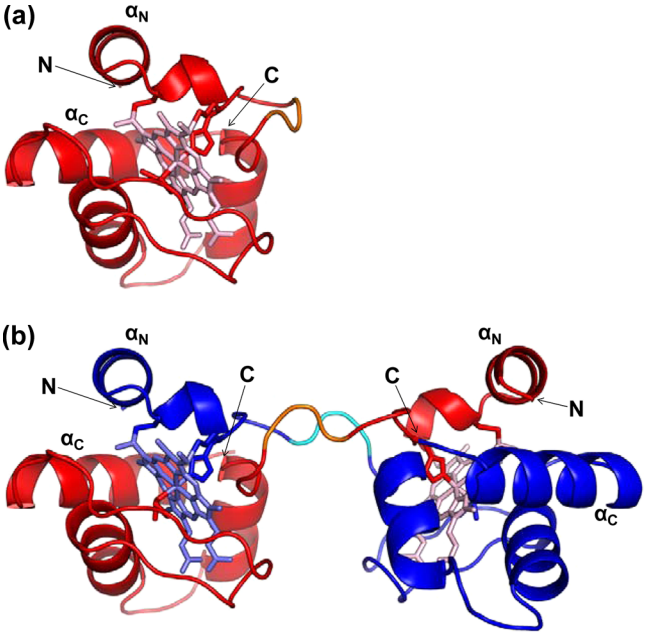

Figure 2. Crystal structures of monomeric and dimeric HT cyt c_{552}. (A) Structure of monomeric HT cyt c_{552} reported previously (PDB: 1YNR). (B) Structure of dimeric HT cyt c_{552} (red and blue). The hemes are shown as pink and slate blue stick models. Side-chain atoms of His14 and Met59 are shown as stick models. The N- and C-termini and the N- and C-terminal helices are labeled as N, C, α_N, and α_C, respectively. The Ala18−Lys20 residues (hinge loop) are depicted in orange and cyan.

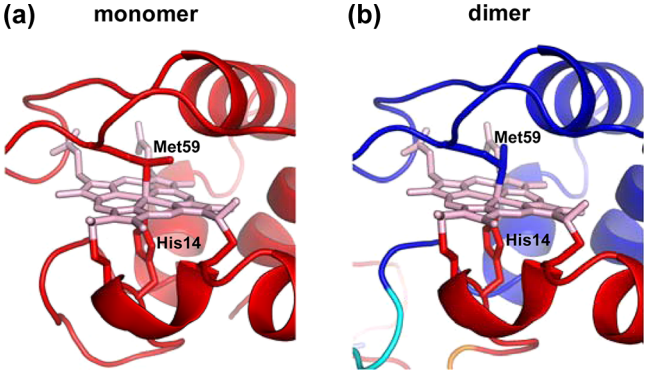

Figure 3. Active site structures of monomeric and dimeric HT cyt c_{552}. (A) Structure of monomeric HT cyt c_{552} (PDB: 1YNR). (B) Structure of dimeric HT cyt c_{552} solved in this study. The red and blue strands in the dimeric structure are regions from different protomers. Side-chain atoms of His14 and Met59 are shown as stick models.

Table 1. Fe−His14 and Fe−Met59 Distances in Monomeric and Dimeric HT cyt c_{552}

	Fe−His14 (Å)	Fe−Met59 (Å)
dimer	1.89	2.28
monomer[a]	2.09	2.40
	2.05	2.33
	2.06	2.34
	2.05	2.33

[a]PDB: 1YNR. There are four independent HT cyt c_{552} molecules in the asymmetric unit of the monomeric HT cyt c_{552} crystal.

(Figure S3, Supporting Information). We have calculated the root-mean-square deviation (rmsd) values of the N-terminal α-helical region including the heme and the rest of the protein (excluding the hinge loop) between the structures of the monomer (four molecules in the asymmetric unit) and the protomer of the dimer (Table S2, Supporting Information). The rmsd values of both the N-terminal region (Asn1−Lys17) with the heme and the rest of the protein (Val21−Lys80) between the protomer of the dimer and the monomer (calculated for each molecule in the asymmetric unit) were 0.43−0.58 and 0.32−0.41, respectively. These results indicate that the structures of the N-terminal region are similar between the monomer and the protomer of the dimer, as well as the rest of the protein excluding the hinge loop (Ala18−Lys20).

Most of the interactions in the monomer were maintained in the dimer. However, the hydrogen bonds (<3.2 Å between heavy atoms) at or near the hinge loop (Ala18−Lys20) in the monomer (Asp15(Oδ2)/Lys17(N), Asp15(Oδ2)/Ala18(N), Lys19(Nζ)/Asp27(Oδ1)) are broken in the dimer, and a new hydrogen bond $Asp15_A(O\delta1)/Lys20_B(N\zeta)$ (and $Lys20_A(N\zeta)/Asp15_B(O\delta1)$) (A and B represent each protomer) is created between the protomers (Figure S4, Supporting Information). This new hydrogen bond may stabilize the dimeric structure. Interestingly, the hydrogen bonds Leu16(O)/Ala26 (N) and Met11(O)/Lys20(Nζ), which are positioned at or near the Ala18−Lys20 region in the monomer, are formed between different protomers in the dimer (Figure S4, Supporting Information). The packing of Ala5, Met11, Tyr32, Tyr41, and Ile76 in monomeric HT cyt c_{552} has been shown to be important for its thermostability.[28−31] In the dimer, the positions of these residues are maintained, although Ala5 and Met11 originate from one protomer and Tyr32, Tyr41, and Ile76 originate from the other protomer to construct a tight structure similar to the monomer (Figure S5, Supporting Information).

Redox Potential of Dimeric HT Cyt c_{552}. We measured the cyclic voltammograms of monomeric and dimeric HT cyt c_{552} to compare their redox potentials. The E_m of dimeric HT cyt c_{552} shifted to a slightly lower potential at 213 ± 2 mV compared to that of the monomer at 240 ± 2 mV (Figure 4).

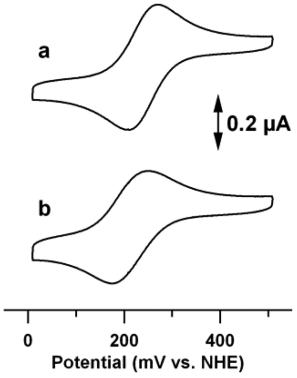

Figure 4. Cyclic voltammograms of monomeric (a) and dimeric (b) HT cyt c_{552}. Measurement conditions: Sample concentration: 200 μM (heme); scan rate: 50 mV/s; temperature: room temperature.

The small shift (−27 mV) in the redox potential on dimerization of HT cyt c_{552} may be attributed to the small change in the active site structure on dimerization. The shorter Fe−His14 and Fe−Met59 bond lengths may cause stronger electron donation from the ligands to the heme iron, resulting in a shift to a lower potential (Table 1), whereas a change in the solvent accessibility of the heme site may also affect the redox

dx.doi.org/10.1021/bi3011303 | Biochemistry 2012, 51, 8608−8616

potential.[53,54] However, the shift in the redox potential on dimerization was relatively small and the high redox potential was maintained in the dimer, due to the active site structure and the protein structure surrounding the heme propionates of the dimer being similar to those of the monomer.

Thermostability and Thermodynamics of Dimeric HT cyt c_{552}. Oxidized dimeric HT cyt c_{552} did not dissociate to monomers by incubation at 70 °C for 5 min (Figure S6, curve b, Supporting Information), while oxidized dimeric horse cyt *c* dissociated to monomers under the same conditions.[22] No more than half the dimeric HT cyt c_{552} dissociated by incubation at 90 °C for 5 min (Figure S6, curve c, Supporting Information). These results show that dimeric HT cyt c_{552} possesses a thermostability as high as its monomer.

The activation enthalpy ($\Delta H^{\ddagger}$) and activation entropy ($\Delta S^{\ddagger}$) for the dissociation of oxidized dimeric HT cyt c_{552} to monomers were obtained from the Eyring plot of $\ln(k/T)$ vs. the reciprocal of temperature (Figure 5). From the plot, $\Delta H^{\ddagger}$ and $\Delta S^{\ddagger}$ for the dissociation of the dimer were calculated from the slope and y-intercept, which were obtained as 140 ± 9 kcal/mol and 310 ± 30 cal/(mol·K), respectively, in the absence of ethanol. In the presence of 60% ethanol, $\Delta H^{\ddagger}$ and $\Delta S^{\ddagger}$ decreased to 110 ± 5 kcal/mol and 270 ± 20 cal/(mol·K), respectively.

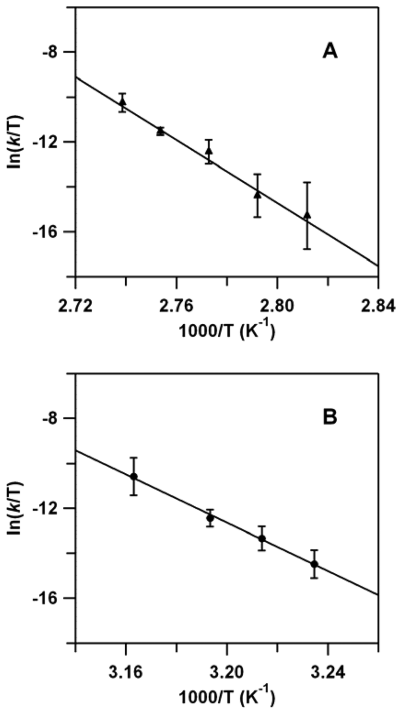

Figure 5. Plots of $\ln(k/T)$ vs. reciprocal of temperature on dissociation of dimeric HT cyt c_{552} in the (A) absence and (B) presence of 60% (v/v) ethanol. The linear lines are obtained by least-squares fitting the plots. Reaction conditions: Sample concentration: 10 μM (heme); solvent: 50 mM sodium phosphate buffer; pH: 7.0; temperature: (A) 82.5–92 °C, (B) 36–43 °C.

DSC measurements for oxidized monomeric and dimeric HT cyt c_{552} were performed to reveal the thermodynamic properties of dimeric HT cyt c_{552} in more detail (Figure 6). The peak temperature (T_m) at 92.3 ± 0.3 °C corresponds to the dissociation temperature of the dimer, since mostly monomers were detected by gel chromatographic analysis after the dimers were scanned up to 95 °C with the DSC equipment. No peak was observed at 90–95 °C in the DSC curve of the monomer. The peak area represents the enthalpy change (ΔH) for the dissociation of the dimer to monomers. ΔH for the dissociation of the dimer exhibited a positive value, 14 ± 2 kcal/mol, indicating that dimeric HT cyt c_{552} is enthalpically favored compared to its monomer, although dimeric horse cyt *c* is enthalpically disfavored compared to its monomer.[22]

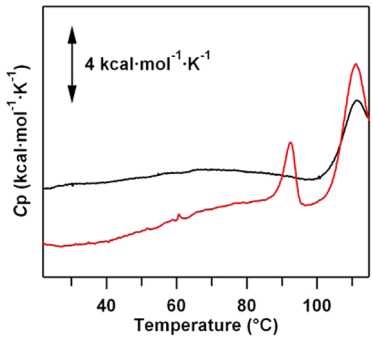

Figure 6. Differential scanning calorimetry thermograms of oxidized monomeric (black) and dimeric (red) HT cyt c_{552}. Measurement conditions: Sample concentration: 100 μM (heme); buffer: 50 mM sodium phosphate buffer; pH: 7.0.

Effect of Ethanol on HT Cyt c_{552} Structure. We investigated the effect of ethanol on the structure of oxidized HT cyt c_{552}, since the oligomers of HT cyt c_{552} were produced by interaction with ethanol (Figure S1, Supporting Information), as well as it enhanced dissociation of dimeric HT cyt c_{552} to monomers (Figure 5 and Figure S2, Supporting Information). Although no distinct change was observed in the absorption spectra of oxidized HT cyt c_{552} by interaction with 60% (v/v) ethanol at 20 °C or without ethanol at 50 °C, the intensity of the 690-nm absorption band decreased by interaction with 60% (v/v) ethanol at 50 °C (Figure S7, Supporting Information). These results show that the Met coordination to the heme iron in oxidized HT cyt c_{552} is perturbed with addition of ethanol at 50 °C but not at 20 °C. In fact, HT cyt c_{552} oligomers were detected more in the precipitates obtained by addition of ethanol at higher temperatures (Figure S1, Supporting Information). However, no dimeric HT cyt c_{552} was detected from the protein solution with addition of 60% (v/v) ethanol at 20 and 50 °C (Figure S8, Supporting Information).

DISCUSSION

HT cyt c_{552} formed a dimer by domain swapping its N-terminal α-helix containing the heme with another HT cyt c_{552} molecule (Figure 2). Met and His residues coordinated to the heme iron in dimeric HT cyt c_{552}, but they originated from different protomers (Figure 3). An exchanged heme ligand has been observed for the *b*-type heme in dimeric hemophore HasA.[16] These results indicate that the heme may exchange its ligand between different molecules of the same protein, forming domain-swapped dimers. The redox potential of domain-swapped dimeric HT cyt c_{552} was obtained as 213 ± 2 mV. The high redox potential was maintained in the dimer, due to the Met and His coordination to the heme in the dimer. Recently, domain-swapped dimeric myoglobin has been shown to possess a similar active site structure and oxygen binding character as those of its monomer.[17] These results show that domain

dx.doi.org/10.1021/bi3011303 | *Biochemistry* 2012, 51, 8608–8616

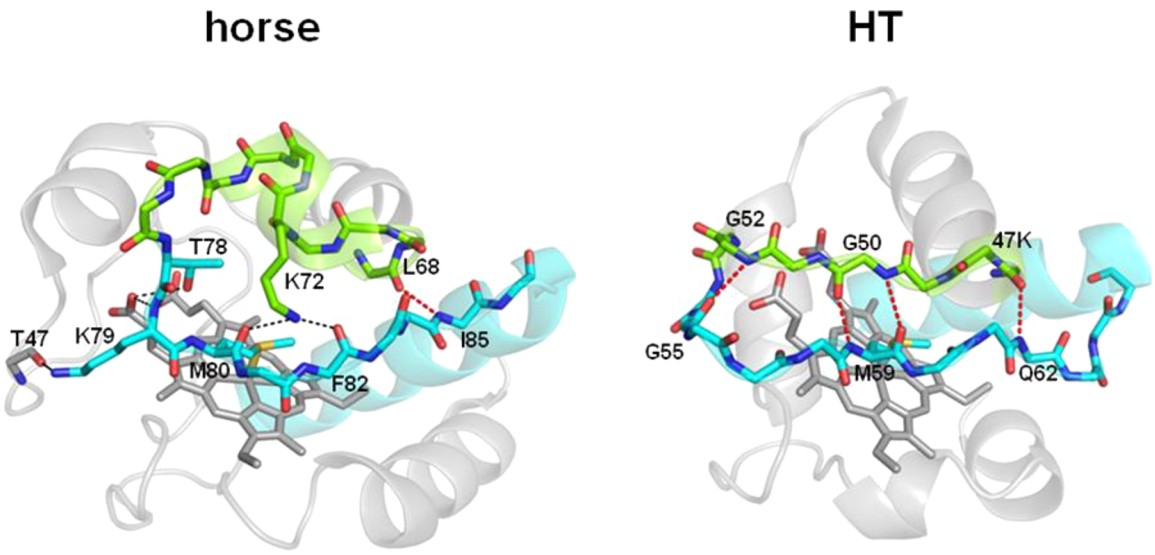

Figure 7. Schematic views of the hydrogen bonds at the loop before the C-terminal α-helix for horse cyt *c* (PDB: 1HRC) and HT cyt c_{552} (PDB: 1YNR). The loops containing the heme-coordinating Met residue are shown as stick models in green and cyan. The C-terminal α-helix is also depicted in cyan. Hemes are shown as gray stick models. Hydrogen bonds between the backbone atoms are depicted in red broken lines, whereas other hydrogen bonds are depicted in black broken lines. The nitrogen, oxygen, and sulfur atoms are depicted in blue, red, and yellow, respectively.

swapping may be useful to design oligomeric proteins with similar characteristics as their monomers.

The C-terminal α-helical region swapped in dimeric and trimeric horse cyt *c*,[22] whereas the N-terminal α-helical region and the heme swapped in dimeric HT cyt c_{552} (Figure 2). The conformation of Lys20 is slightly distorted in monomeric HT cyt c_{552}. Backbone dihedral angles of dimeric HT cyt c_{552} are (φ, ψ) = (−95.7°, 144.8°)), whereas (φ, ψ) are (−98.5°, −122.3°), (−108.6°, −83.7°), (−100.9°, −125.8°), and (−114.3°, −90.6°) for the four molecules in the asymmetric unit of the crystal of the monomer. In the Ramachandran plot, the dihedral angle pair (φ, ψ) of Lys20 of the monomer is in the allowed region, whereas that of the dimer is in the favored region (Figure S9, Supporting Information).[55] The structure at the hinge loop (Ala18−Lys20) of the monomer was relocated in the dimer, and the distortion at Lys20 was removed in the dimer.

We have shown that oxidized horse cyt *c* forms domain-swapped oligomers by interaction with ethanol, and that the C-terminal α-helix is swapped in the oligomers.[22] The local protein region around Met80 in cyt *c* has been shown to unfold by benzyl alcohol or *m*-cresol and acts as a "hot spot" for triggering aggregation.[56,57] The loop constructed of the Asn70−Ile85 amino acids has been shown to open first during unfolding of cyt *c*.[58] The Thr78−Lys87 amino acids of the loop of horse cyt *c* form hydrogen bonds (<3.2 Å between heavy atoms) to the rest of the protein at Leu68(O)/Ile85(N), Lys72(Nζ)/Met80(O), Lys72(Nζ)/Phe82(O), Thr78(Oγ)/Hem(O2D), Lys79(N)/Hem(O2D), and Lys79(Nζ)/Thr47(O) in a relatively broad region (Figure 7). On the other hand, the corresponding region (Trp54−Thr65) in monomeric HT cyt c_{552} is fixed to the rest of the protein by forming a β-sheet-like structure with four relatively close hydrogen bonds between the backbone atoms (Lys47(O)/Gln62(N), Gly50(N)/Met59(O), Gly50(O)/Met59(N), and Gly52(N)/Gly55(O)), which creates a relatively tight structure for the amino acids Trp54−Thr65 in the loop (Figure 7). Actually, the Gly50−Met59 residues of HT cyt c_{552} have been suggested to form a short but persistent region of β-sheet secondary structure for its heme-depleted apo state according to molecular dynamic simulation.[59] In addition, relatively strong hydrophobic interactions between Ala73 in the C-terminal α-helix and Val39, Leu42, Ala43, and Ile46 in the neighboring α-helix (Ala38−Lys48) exist in HT cyt c_{552}, whereas such interaction is not seen in horse cyt *c* (Figure S10, Supporting Information). Therefore, to form dimeric HT cyt c_{552}, the C-terminal α-helix may not exchange its position with the corresponding helix of another molecule and instead, the N-terminal α-helix with the heme may swap between protomers.

Although higher order oligomers were detected in horse cyt *c*, oligomers only up to pentamers were detected in HT cyt c_{552}. The hinge loop, which changes its conformation by domain swapping, consists of only three residues in HT cyt c_{552} (Ala18, Lys19, and Lys20) (Figure S11, Supporting Information), whereas it is relatively long in cyt *c* (Thr78−Lys87). Since the swapping loop is short in HT cyt c_{552}, HT cyt c_{552} oligomers may be subjected to more steric hindrance at the swapped site compared to horse cyt *c*, and thus formation of higher order oligomers may be prevented in HT cyt c_{552}.

The dimers of horse cyt *c* dissociated to monomers when heated at 70 °C for 5 min,[22] whereas dimeric HT cyt c_{552} did not dissociate under the same conditions (Figure S6, Supporting Information). These results show that dimeric HT cyt c_{552} possesses a higher thermostability against dissociation to monomers compared to those of dimeric horse cyt *c*. Comparative studies on homologous proteins from thermophiles and mesophiles have been performed to understand the relationship between protein structure and thermostability,[26,60−67] and the packing by hydrophobic interactions with the surrounding protein for Ala5, Met11, Tyr32, Tyr41, and Ile76 residues has been shown to be important for the thermostability of monomeric HT cyt c_{552}.[28−31] The packing around the side chains of these residues was maintained in dimeric HT cyt c_{552} (Figure S4, Supporting Information), and thus the thermostability of the dimer against dissociation to monomers was high. We attribute the stability of dimeric HT cyt c_{552} to the conserved packing of the amino acid residues responsible for the thermo stability, as in the monomer.

dx.doi.org/10.1021/bi3011303 | *Biochemistry* 2012, 51, 8608−8616

A high activation enthalpy has been obtained for domain-swapped stefin A, p13suc1, and cyanovirin-N, suggesting that domain swapping proceeds via complete unfolding.[39,68,69] It has also been shown that RNase A oligomers are formed by refolding from a chiefly denatured state,[46] where the amounts of the two N-terminal and C-terminal dimers depended on the unfolding conditions.[70] Our results also show that dissociation occurs with a high activation enthalpy in dimeric HT cyt c_{552} (Figure 5). Dimeric HT cyt c_{552} and dimeric horse cyt c dissociate to monomers when heated over 90 and 70 °C, respectively. However, ΔH for the dissociation of dimeric HT cyt c_{552} to monomers was positive, whereas ΔH for the dissociation of dimeric horse cyt c was negative.[22] The stronger coordination of the His and Met ligands to the heme iron in dimeric HT cyt c_{552} compared to the monomer (Table 1) and the removal of the stress around Lys20 in the dimer (Figure S9, Supporting Information) may contribute to ΔH for the dissociation exhibiting a positive value. On the other hand, Met dissociated from the heme iron in the dimer and trimer, and the loop before the C-terminal α-helix was long and relatively flexible in the monomer for horse cyt c. These results show the diversity in the properties of domain swapping even between the proteins in the same superfamily.

For domain swapping of HT cyt c_{552} with addition of ethanol, it may be important for the N-terminal α-helix to conserve its α-helical structure. In fact, trifluoroethanol promotes helical formation in the sequences that have a tendency to be helical in solution.[71,72] Since the Met-heme iron bond needs to cleave to form a domain-swapped oligomer according to its crystal structure (Figure 3), perturbation in the Met coordination seems to be necessary for formation of domain-swapped oligomers. Ethanol induced perturbation in the coordination structure of Met59 to the heme iron in HT cyt c_{552} at relatively high temperatures (Figure S7, Supporting Information), at which oligomerization occurred by domain swapping (Figure S1, Supporting Information). With addition of ethanol to dimeric HT cyt c_{552}, dissociation of the dimer to monomers was also observed (Figure S2, Supporting Information). These results indicate that the structural perturbation with ethanol enhances both association of monomers and dissociation of dimers, probably by decreasing the activation energy. By addition of ethanol, $\Delta H^{\ddagger}$ for dissociation of dimeric HT cyt c_{552} decreased about 30 kcal/mol, showing that ethanol reduces the activation energy for the dissociation of the dimer. Met dissociates from the heme by addition of ethanol (Figure S7, Supporting Information), which may cause a decrease in the $\Delta H^{\ddagger}$ value. Actually, the enthalpy change upon Met coordination to the heme in cyt c has been estimated to be −18 kcal/mol.[73] Although the swapping region in the proteins of the cyt c superfamily differ,[22] ethanol enhances formation of both dimeric HT cyt c_{552} and dimeric horse cyt c by dissociation of Met from the heme iron. These properties may be a common feature in domain swapping of proteins in the cyt c superfamily.

Met dissociation from the heme iron has been mentioned to be important for apoptosis and the peroxidase activity of cyt c.[23,74,75] Since the Met dissociation is observed in dimeric and oligomeric horse cyt c[22] but not in dimeric HT cyt c_{552}, the Met dissociation ability of horse cyt c may be related to its apoptotic function.

CONCLUSION

HT cyt c_{552} formed a domain-swapped dimer by treatment with ethanol. However, the domain-swapped region in dimeric HT cyt c_{552} was different from that in dimeric horse cyt c. The N-terminal α-helix together with the heme was exchanged in dimeric HT cyt c_{552}, whereas the C-terminal α-helix was exchanged in dimeric horse cyt c. The loop region at Trp54–Thr65 in monomeric HT cyt c_{552} is fixed to the rest of the protein by forming a β-sheet-like structure, which may inhibit the C-terminal α-helix from dissociating from the rest of the protein. The heme iron was six-coordinate in dimeric HT cyt c_{552}, but the coordinated Met originated from the other protomer to which the heme belonged. Dimeric HT cyt c_{552} exhibited high thermostability, due to the similar packing around the side chains of the residues important for the thermostability as in the monomer. Dissociation of dimeric HT cyt c_{552} to monomers exhibited high activation enthalpy $\Delta H^{\ddagger}$ (140 ± 9 kcal/mol) and activation entropy $\Delta S^{\ddagger}$ (310 ± 30 cal/(mol·K)). Ethanol may enhance formation of domain-swapped oligomers for the proteins in the cyt c superfamily by dissociating Met from the heme iron and decreasing the activation energy, although the swapping region may differ. These results show that domain swapping may be a common phenomenon in heme proteins, although the swapping region may differ and depend on the relative flexibility of the swapping region against the rest of the protein.

ASSOCIATED CONTENT

Supporting Information

Statistics of data collection, root-mean-square deviation values, size exclusion chromatography, structures, absorption spectra, and Ramachandran plots are included as Supporting Information. This material is available free of charge via the Internet at http://pubs.acs.org.

AUTHOR INFORMATION

Corresponding Author

*Phone: +81-743-72-6110. Fax: +81-743-72-6119. E-mail: hirota@ms.naist.jp.

Funding

This work was partially supported by Grants-in-Aid for Scientific Research from MEXT (Priority Areas, No. 23107723 (S.H.)), JSPS (Category B No. 21350095 (S.H.)), Sankyo Foundation of Life Science (S.H.), and Toray Science Foundation (S.H.).

Notes

The authors declare no competing financial interest.

ACKNOWLEDGMENTS

We thank Prof. Yoshihiro Sambongi, Hiroshima University, for a kind gift of pKO2 and pEC86 plasmids carrying the genes for HT cyt c_{552} and cytochrome c maturation proteins, respectively. We are also grateful to Mr. Leigh McDowell, Nara Institute of Science and Technology, for his advice on manuscript preparation.

ABBREVIATIONS USED

cyt c, cytochrome c; HT, *Hydrogenobacter thermophilus*; cyt c_{552}, cytochrome c_{552}; T_d, denaturation temperature; PA, *Pseudomonas aeruginosa*; cyt c_{551}, cytochrome c_{551}; E_m, midpoint redox potential; CD, circular dichroism; NHE, normal hydrogen electrode; DSC, differential scanning calorimetry; rmsd, root-

mean-square deviation; $\Delta H^{\ddagger}$, activation enthalpy; $\Delta S^{\ddagger}$, activation entropy; T_m, peak temperature; ΔH, enthalpy change

REFERENCES

(1) Anfinsen, C. B. (1973) Principles that govern the folding of protein chains. *Science 181*, 223−230.

(2) Bucciantini, M., Giannoni, E., Chiti, F., Baroni, F., Formigli, L., Zurdo, J., Taddei, N., Ramponi, G., Dobson, C. M., and Stefani, M. (2002) Inherent toxicity of aggregates implies a common mechanism for protein misfolding diseases. *Nature 416*, 507−511.

(3) Kayed, R., Head, E., Thompson, J. L., McIntire, T. M., Milton, S. C., Cotman, C. W., and Glabe, C. G. (2003) Common structure of soluble amyloid oligomers implies common mechanism of pathogenesis. *Science 300*, 486−489.

(4) Chiti, F., and Dobson, C. M. (2009) Amyloid formation by globular proteins under native conditions. *Nat. Chem. Biol. 5*, 15−22.

(5) Bennett, M. J., Sawaya, M. R., and Eisenberg, D. (2006) Deposition diseases and 3D domain swapping. *Structure 14*, 811−824.

(6) Nelson, R., and Eisenberg, D. (2006) Recent atomic models of amyloid fibril structure. *Curr. Opin. Struct. Biol. 16*, 260−265.

(7) Knaus, K. J., Morillas, M., Swietnicki, W., Malone, M., Surewicz, W. K., and Yee, V. C. (2001) Crystal structure of the human prion protein reveals a mechanism for oligomerization. *Nat. Struct. Biol. 8*, 770−774.

(8) Guo, Z., and Eisenberg, D. (2006) Runaway domain swapping in amyloid-like fibrils of T7 endonuclease I. *Proc. Natl. Acad. Sci. U.S.A. 103*, 8042−8047.

(9) Liu, C., Sawaya, M. R., and Eisenberg, D. (2011) β_2-microglobulin forms three-dimensional domain-swapped amyloid fibrils with disulfide linkages. *Nat. Struct. Mol. Biol. 18*, 49−55.

(10) Janowski, R., Kozak, M., Jankowska, E., Grzonka, Z., Grubb, A., Abrahamson, M., and Jaskolski, M. (2001) Human cystatin C, an amyloidogenic protein, dimerizes through three-dimensional domain swapping. *Nat. Struct. Biol. 8*, 316−320.

(11) Newcomer, M. E. (2002) Protein folding and three-dimensional domain swapping: a strained relationship? *Curr. Opin. Struct. Biol. 12*, 48−53.

(12) Rousseau, F., Schymkowitz, J. W., and Itzhaki, L. S. (2003) The unfolding story of three-dimensional domain swapping. *Structure 11*, 243−251.

(13) Gronenborn, A. M. (2009) Protein acrobatics in pairs−dimerization via domain swapping. *Curr. Opin. Struct. Biol. 19*, 39−49.

(14) Nurizzo, D., Silvestrini, M. C., Mathieu, M., Cutruzzolà, F., Bourgeois, D., Fülöp, V., Hajdu, J., Brunori, M., Tegoni, M., and Cambillau, C. (1997) N-terminal arm exchange is observed in the 2.15 Å crystal structure of oxidized nitrite reductase from *Pseudomonas aeruginosa*. *Structure 5*, 1157−1171.

(15) Crane, B. R., Rosenfeld, R. J., Arvai, A. S., Ghosh, D. K., Ghosh, S., Tainer, J. A., Stuehr, D. J., and Getzoff, E. D. (1999) N-terminal domain swapping and metal ion binding in nitric oxide synthase dimerization. *EMBO J. 18*, 6271−6281.

(16) Czjzek, M., Létoffé, S., Wandersman, C., Delepierre, M., Lecroisey, A., and Izadi-Pruneyre, N. (2007) The crystal structure of the secreted dimeric form of the hemophore HasA reveals a domain swapping with an exchanged heme ligand. *J. Mol. Biol. 365*, 1176−1186.

(17) Nagao, S., Osuka, H., Yamada, T., Uni, T., Shomura, Y., Imai, K., Higuchi, Y., and Hirota, S. (2012) Structural and oxygen binding properties of dimeric horse myoglobin. *Dalton Trans. 41*, 11378−11385.

(18) Yamasaki, M., Li, W., Johnson, D. J., and Huntington, J. A. (2008) Crystal structure of a stable dimer reveals the molecular basis of serpin polymerization. *Nature 455*, 1255−1258.

(19) Yamasaki, M., Sendall, T. J., Pearce, M. C., Whisstock, J. C., and Huntington, J. A. (2011) Molecular basis of α1-antitrypsin deficiency revealed by the structure of a domain-swapped trimer. *EMBO Rep. 12*, 1011−1017.

(20) Sambashivan, S., Liu, Y., Sawaya, M. R., Gingery, M., and Eisenberg, D. (2005) Amyloid-like fibrils of ribonuclease A with three-dimensional domain-swapped and native-like structure. *Nature 437*, 266−269.

(21) Das, P., King, J. A., and Zhou, R. (2011) Aggregation of γ-crystallins associated with human cataracts via domain swapping at the C-terminal β-strands. *Proc. Natl. Acad. Sci. U.S.A. 108*, 10514−10519.

(22) Hirota, S., Hattori, Y., Nagao, S., Taketa, M., Komori, H., Kamikubo, H., Wang, Z., Takahashi, I., Negi, S., Sugiura, Y., Kataoka, M., and Higuchi, Y. (2010) Cytochrome *c* polymerization by successive domain swapping at the C-terminal helix. *Proc. Natl. Acad. Sci. U.S.A. 107*, 12854−12859.

(23) Wang, Z., Matsuo, T., Nagao, S., and Hirota, S. (2011) Peroxidase activity enhancement of horse cytochrome *c* by dimerization. *Org. Biomol. Chem. 9*, 4766−4769.

(24) Lopes, H., Besson, S., Moura, I., and Moura, J. J. (2001) Kinetics of inter- and intramolecular electron transfer of *Pseudomonas nautica* cytochrome cd_1 nitrite reductase: regulation of the NO-bound end product. *J. Biol. Inorg. Chem. 6*, 55−62.

(25) Travaglini-Allocatelli, C., Gianni, S., Dubey, V. K., Borgia, A., Di Matteo, A., Bonivento, D., Cutruzzolà, F., Bren, K. L., and Brunori, M. (2005) An obligatory intermediate in the folding pathway of cytochrome c_{552} from *Hydrogenobacter thermophilus*. *J. Biol. Chem. 280*, 25729−25734.

(26) Hasegawa, J., Yoshida, T., Yamazaki, T., Sambongi, Y., Yu, Y., Igarashi, Y., Kodama, T., Yamazaki, K., Kyogoku, Y., and Kobayashi, Y. (1998) Solution structure of thermostable cytochrome *c*-552 from *Hydrogenobacter thermophilus* determined by ^{1}H-NMR spectroscopy. *Biochemistry 37*, 9641−9649.

(27) Yamamoto, Y., Terui, N., Tachiiri, N., Minakawa, K., Matsuo, H., Kameda, T., Hasegawa, J., Sambongi, Y., Uchiyama, S., Kobayashi, Y., and Igarashi, Y. (2002) Influence of amino acid side chain packing on Fe-methionine coordination in thermostable cytochrome *c*. *J. Am. Chem. Soc. 124*, 11574−11575.

(28) Hasegawa, J., Shimahara, H., Mizutani, M., Uchiyama, S., Arai, H., Ishii, M., Kobayashi, Y., Ferguson, S. J., Sambongi, Y., and Igarashi, Y. (1999) Stabilization of Pseudomonas aeruginosa cytochrome c_{551} by systematic amino acid substitutions based on the structure of thermophilic *Hydrogenobacter thermophilus* cytochrome c_{552}. *J. Biol. Chem. 274*, 37533−37537.

(29) Hasegawa, J., Uchiyama, S., Tanimoto, Y., Mizutani, M., Kobayashi, Y., Sambongi, Y., and Igarashi, Y. (2000) Selected mutations in a mesophilic cytochrome *c* confer the stability of a thermophilic counterpart. *J. Biol. Chem. 275*, 37824−37828.

(30) Uchiyama, S., Hasegawa, J., Tanimoto, Y., Moriguchi, H., Mizutani, M., Igarashi, Y., Sambongi, Y., and Kobayashi, Y. (2002) Thermodynamic characterization of variants of mesophilic cytochrome *c* and its thermophilic counterpart. *Protein Eng. 15*, 455−462.

(31) Oikawa, K., Nakamura, S., Sonoyama, T., Ohshima, A., Kobayashi, Y., Takayama, S. J., Yamamoto, Y., Uchiyama, S., Hasegawa, J., and Sambongi, Y. (2005) Five amino acid residues responsible for the high stability of *Hydrogenobacter thermophilus* cytochrome c_{552}: reciprocal mutation analysis. *J. Biol. Chem. 280*, 5527−5532.

(32) Takahashi, Y. T., Sasaki, H., Takayama, S. J., Mikami, S., Kawano, S., Mita, H., Sambongi, Y., and Yamamoto, Y. (2006) Further enhancement of the thermostability of *Hydrogenobacter thermophilus* cytochrome c_{552}. *Biochemistry 45*, 11005−11011.

(33) Tai, H., Irie, K., Mikami, S., and Yamamoto, Y. (2011) Enhancement of the thermostability of *Hydrogenobacter thermophilus* cytochrome c_{552} through introduction of an extra methylene group into its hydrophobic protein interior. *Biochemistry 50*, 3161−3169.

(34) Terui, N., Tachiiri, N., Matsuo, H., Hasegawa, J., Uchiyama, S., Kobayashi, Y., Igarashi, Y., Sambongi, Y., and Yamamoto, Y. (2003) Relationship between redox function and protein stability of cytochromes *c*. *J. Am. Chem. Soc. 125*, 13650−13651.

(35) Pertinhez, T. A., Bouchard, M., Tomlinson, E. J., Wain, R., Ferguson, S. J., Dobson, C. M., and Smith, L. J. (2001) Amyloid fibril formation by a helical cytochrome. *FEBS Lett. 495*, 184−186.

(36) de Groot, N. S., and Ventura, S. (2005) Amyloid fibril formation by bovine cytochrome *c*. *Spectroscopy 19*, 199−205.

(37) Bennett, M. J., Choe, S., and Eisenberg, D. (1994) Domain swapping: entangling alliances between proteins. *Proc. Natl. Acad. Sci. U.S.A. 91*, 3127−3131.
(38) Bennett, M. J., Schlunegger, M. P., and Eisenberg, D. (1995) 3D domain swapping: a mechanism for oligomer assembly. *Protein Sci. 4*, 2455−2468.
(39) Rousseau, F., Schymkowitz, J. W., Wilkinson, H. R., and Itzhaki, L. S. (2001) Three-dimensional domain swapping in p13suc1 occurs in the unfolded state and is controlled by conserved proline residues. *Proc. Natl. Acad. Sci. U.S.A. 98*, 5596−5601.
(40) Schymkowitz, J. W., Rousseau, F., Wilkinson, H. R., Friedler, A., and Itzhaki, L. S. (2001) Observation of signal transduction in three-dimensional domain swapping. *Nat. Struct. Biol. 8*, 888−892.
(41) Barrientos, L. G., Louis, J. M., Botos, I., Mori, T., Han, Z., O'Keefe, B. R., Boyd, M. R., Wlodawer, A., and Gronenborn, A. M. (2002) The domain-swapped dimer of cyanovirin-N is in a metastable folded state: reconciliation of X-ray and NMR structures. *Structure 10*, 673−686.
(42) Chen, Y. W., Stott, K., and Perutz, M. F. (1999) Crystal structure of a dimeric chymotrypsin inhibitor 2 mutant containing an inserted glutamine repeat. *Proc. Natl. Acad. Sci. U.S.A. 96*, 1257−1261.
(43) Liu, Y., Gotte, G., Libonati, M., and Eisenberg, D. (2002) Structures of the two 3D domain-swapped RNase A trimers. *Protein Sci. 11*, 371−380.
(44) Liu, Y., Hart, P. J., Schlunegger, M. P., and Eisenberg, D. (1998) The crystal structure of a 3D domain-swapped dimer of RNase A at a 2.1-Å resolution. *Proc. Natl. Acad. Sci. U.S.A. 95*, 3437−3442.
(45) Liu, Y., Gotte, G., Libonati, M., and Eisenberg, D. (2001) A domain-swapped RNase A dimer with implications for amyloid formation. *Nat. Struct. Biol. 8*, 211−214.
(46) López-Alonso, J. P., Bruix, M., Font, J., Ribó, M., Vilanova, M., Jiménez, M. A., Santoro, J., González, C., and Laurents, D. V. (2010) NMR spectroscopy reveals that RNase A is chiefly denatured in 40% acetic acid: implications for oligomer formation by 3D domain swapping. *J. Am. Chem. Soc. 132*, 1621−1630.
(47) Berry, E. A., and Trumpower, B. L. (1987) Simultaneous determination of hemes *a*, *b*, and *c* from pyridine hemochrome spectra. *Anal. Biochem. 161*, 1−15.
(48) Otwinowski, Z., and Minor, W. (1997) Processing of X-ray diffraction data collected in oscillation mode. *Methods Enzymol 276*, 307−326.
(49) Battistuzzi, G., Borsari, M., Sola, M., and Francia, F. (1997) Redox thermodynamics of the native and alkaline forms of eukaryotic and bacterial class I cytochromes *c*. *Biochemistry 36*, 16247−16258.
(50) Ishii, M., Igarashi, Y., and Kodama, T. (1987) Purification and some properties of cytochrome c_{552} from *Hydrogenobacter thermophilus*. *Agric. Biol. Chem. 51*, 1695−1696.
(51) Wen, X., and Bren, K. L. (2005) Suppression of axial methionine fluxion in Hydrogenobacter thermophilus Gln64Asn cytochrome c_{552}. *Biochemistry 44*, 5225−5233.
(52) Karan, E. F., Russell, B. S., and Bren, K. L. (2002) Characterization of Hydrogenobacter thermophilus cytochromes c_{552} expressed in the cytoplasm and periplasm of *Escherichia coli*. *J. Biol. Inorg. Chem. 7*, 260−272.
(53) Moore, G. R., Pettigrew, G. W., and Rogers, N. K. (1986) Factors influencing redox potentials of electron transfer proteins. *Proc. Natl. Acad. Sci. U.S.A. 83*, 4998−4999.
(54) Tezcan, F. A., Winkler, J. R., and Gray, H. B. (1998) Effects of ligation and folding on reduction potentials of heme proteins. *J. Am. Chem. Soc. 120*, 13383−13388.
(55) Lovell, S. C., Davis, I. W., Arendall, W. B., 3rd, de Bakker, P. I., Word, J. M., Prisant, M. G., Richardson, J. S., and Richardson, D. C. (2003) Structure validation by Cα geometry: φ, ψ and Cβ deviation. *Proteins 50*, 437−450.
(56) Singh, S. M., Cabello-Villegas, J., Hutchings, R. L., and Mallela, K. M. (2010) Role of partial protein unfolding in alcohol-induced protein aggregation. *Proteins 78*, 2625−2637.
(57) Singh, S. M., Hutchings, R. L., and Mallela, K. M. (2011) Mechanisms of *m*-cresol-induced protein aggregation studied using a model protein cytochrome *c*. *J. Pharm. Sci. 100*, 1679−1689.
(58) Bai, Y., Sosnick, T. R., Mayne, L., and Englander, S. W. (1995) Protein folding intermediates: native-state hydrogen exchange. *Science 269*, 192−197.
(59) Smith, L. J., Davies, R. J., and van Gunsteren, W. F. (2006) Molecular dynamics simulations of *Hydrogenobacter thermophilus* cytochrome c_{552}: comparisons of the wild-type protein, a *b*-type variant, and the apo state. *Proteins 65*, 702−711.
(60) Szilágyi, A., and Závodszky, P. (2000) Structural differences between mesophilic, moderately thermophilic and extremely thermophilic protein subunits: results of a comprehensive survey. *Structure 8*, 493−504.
(61) Cambillau, C., and Claverie, J. M. (2000) Structural and genomic correlates of hyperthermostability. *J. Biol. Chem. 275*, 32383−32386.
(62) Ishikawa, K., Okumura, M., Katayanagi, K., Kimura, S., Kanaya, S., Nakamura, H., and Morikawa, K. (1993) Crystal structure of ribonuclease H from Thermus thermophilus HB8 refined at 2.8 Å resolution. *J. Mol. Biol. 230*, 529−542.
(63) Knapp, S., de Vos, W. M., Rice, D., and Ladenstein, R. (1997) Crystal structure of glutamate dehydrogenase from the hyperthermophilic eubacterium *Thermotoga maritima* at 3.0 Å resolution. *J. Mol. Biol. 267*, 916−932.
(64) Knapp, S., Kardinahl, S., Hellgren, N., Tibbelin, G., Schäfer, G., and Ladenstein, R. (1999) Refined crystal structure of a superoxide dismutase from the hyperthermophilic archaeon *Sulfolobus acidocaldarius* at 2.2 Å resolution. *J. Mol. Biol. 285*, 689−702.
(65) Vinther, J. M., Kristensen, S. M., and Led, J. J. (2011) Enhanced stability of a protein with increasing temperature. *J. Am. Chem. Soc. 133*, 271−278.
(66) Hollien, J., and Marqusee, S. (1999) A thermodynamic comparison of mesophilic and thermophilic ribonucleases H. *Biochemistry 38*, 3831−3836.
(67) Razvi, A., and Scholtz, J. M. (2006) Lessons in stability from thermophilic proteins. *Protein Sci. 15*, 1569−1578.
(68) Jerala, R., and Žerovnik, E. (1999) Accessing the global minimum conformation of stefin A dimer by annealing under partially denaturing conditions. *J. Mol. Biol. 291*, 1079−1089.
(69) Liu, L., Byeon, I. J., Bahar, I., and Gronenborn, A. M. (2012) Domain swapping proceeds via complete unfolding: a 19F- and 1H-NMR study of the Cyanovirin-N protein. *J. Am. Chem. Soc. 134*, 4229−4235.
(70) Gotte, G., Vottariello, F., and Libonati, M. (2003) Thermal aggregation of ribonuclease A. A contribution to the understanding of the role of 3D domain swapping in protein aggregation. *J. Biol. Chem. 278*, 10763−10769.
(71) Muñoz, V., and Serrano, L. (1994) Elucidating the folding problem of helical peptides using empirical parameters. *Nat. Struct. Biol. 1*, 399−409.
(72) Storrs, R. W., Truckses, D., and Wemmer, D. E. (1992) Helix propagation in trifluoroethanol solutions. *Biopolymers 32*, 1695−1702.
(73) George, P., Glauser, S. C., and Schejter, A. (1967) The reactivity of ferricytochrome *c* with ionic ligands. *J. Biol. Chem. 242*, 1690−1695.
(74) Kagan, V. E., Tyurin, V. A., Jiang, J., Tyurina, Y. Y., Ritov, V. B., Amoscato, A. A., Osipov, A. N., Belikova, N. A., Kapralov, A. A., Kini, V., Vlasova, I. I., Zhao, Q., Zou, M., Di, P., Svistunenko, D. A., Kurnikov, I. V., and Borisenko, G. G. (2005) Cytochrome *c* acts as a cardiolipin oxygenase required for release of proapoptotic factors. *Nat. Chem. Biol. 1*, 223−232.
(75) Belikova, N. A., Vladimirov, Y. A., Osipov, A. N., Kapralov, A. A., Tyurin, V. A., Potapovich, M. V., Basova, L. V., Peterson, J., Kurnikov, I. V., and Kagan, V. E. (2006) Peroxidase activity and structural transitions of cytochrome *c* bound to cardiolipin-containing membranes. *Biochemistry 45*, 4998−5009.